

Deuterium retention mechanism in tungsten-coatings exposed to JT-60U divertor plasmas

M. Fukumoto 1), T. Nakano 1), K. Itami 1), T. Wada 2), Y. Ueda 2), T. Tanabe3)

1) Japan Atomic Energy Agency, Mukouyama, Naka, Ibaraki-ken 311-0193, Japan

2) Graduate School of Engineering, Osaka University, Suita, Osaka 565-0871, Japan

3) Interdisciplinary Graduate School of Engineering Science, Kyusyu University, Hakozaki, Fukuoka 812-8581, Japan

E-mail contact of main author: fukumoto.masakatsu@jaea.go.jp

Abstract. In the experimental campaign 2003-2004 of JT-60U, twelve tungsten-coated carbon fiber composite tiles were installed at the upper part of divertor tiles and plasma discharges were performed. The deuterium retention in the tungsten-coated tiles was poloidally uniform at $\sim 10^{22}$ D/m². The depth profiles of deuterium concentration in the tungsten coating were similar to that of carbon. This suggests that the incident deuterium is trapped predominantly by the carbon accumulated in the tungsten coating. The origin of the carbon was implantation of eroded carbon from carbon armor tiles. As the result of deuterium trapping to carbon, D/C ratio in the tungsten coating was evaluated to 0.06 ± 0.02 and was 1/2-1/4 for D/C in carbon codeposits formed at similar temperature to the tungsten coating. Comparison of deuterium thermal desorption profile between tungsten-coated tiles exposed to JT-60U divertor plasmas and tungsten-coated samples irradiated with deuterium ion beams indicated that little deuterium would be trapped by monovacancies in the tungsten coating. These results suggest that simultaneous use of carbon and tungsten coating enhances tritium retention in tungsten coating in future deuterium-tritium fusion devices.

1. Introduction

Tungsten is promising candidates for plasma facing materials for future fusion devices. The advantages of tungsten are low hydrogen solubility, low sputtering yield and high melting temperature. In the engineering phase of ITER, it is planned that all the plasma facing components are exchanged to tungsten based materials. Vacuum plasma sputtering (VPS) is one of the methods to cover the large area of the main chamber wall with tungsten. To predict tritium inventory in VPS-W coating, it is necessary to investigate hydrogen isotope behavior such as retention and desorption characteristics. Recently, deuterium retention and desorption characteristics of VPS-W coating were studied by pure deuterium ion beams and plasma simulators [1,2].

Since JT-60U plasma always includes a few % of carbon impurities, tungsten coating would be simultaneously irradiated with tritium and carbon ions. Only 1 % of carbon impurities in hydrogen ions changes the hydrogen retention and desorption characteristics in polycrystalline tungsten [3]. Characteristics of hydrogen isotope behavior in tungsten coating would be also changed by simultaneous irradiation of carbon and hydrogen isotope ions. Therefore, to predict tritium inventory in tungsten coating, it is important to investigate the effects of carbon impurities on deuterium behavior in tungsten coating. In this paper, effects of carbon impurity on deuterium retention and trapping sites for deuterium in tungsten coating exposed to JT-60U divertor plasmas are discussed.

2. Experimental setup

Tungsten with a thickness of ~ 50 μm were coated by VPS on rhenium and tungsten (Re/W) multi-interlayer, which was deposited by physical vapor deposition (PVD) on carbon fiber composite (CFC) substrate.

Figure 1 shows a schematic view of the poloidal cross-section of JT-60U divertor region with typical two types of magnetic configurations. Before the experimental campaign 2003-2004, 12 tungsten-coated CFC tiles were installed in one toroidal section of the upper part of the outer divertor plates. In the experimental campaign, 978 discharges with usual magnetic configurations (red line in Fig. 1) were performed, whereas 25 discharges were operated with a strike point positioned on the tungsten-coated tiles (blue line in Fig.1).

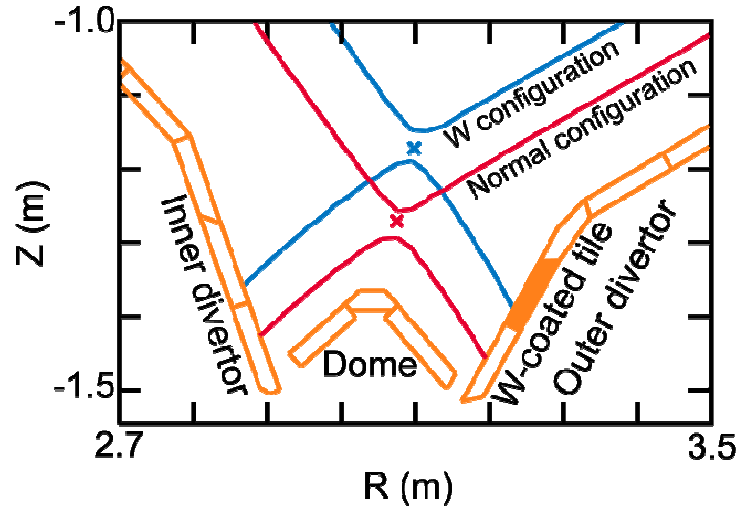


FIG. 1. Poloidal cross-section of JT-60U divertor region with typical separatrix of a usual and a tungsten experimental magnetic configuration. The filled tile shows the tungsten-coated tiles.

Deuterium retention was evaluated with Thermal Desorption Spectroscopy (TDS). The samples were heated from 300 to 1373 K at a heating rate of ~ 0.42 K/s and kept at 1373K for 10 min. Depth profiles of deuterium and carbon in the tungsten coating were obtained by Secondary Ion Mass Spectroscopy (SIMS). Carbon concentration in the tungsten coating was measured by X-ray photoelectron spectroscopy (XPS) with Mg $K\alpha$ radiation. 4 keV argon ion beams were used for depth profiling. The depth of the sputtered crater produced by SIMS and XPS analysis were calibrated by a surface profilometer.

3. Deuterium retention

Figure 2 shows a poloidal distribution of retained deuterium in the tungsten-coated tiles exposed to JT-60U divertor plasmas [4]. The right axis shows a poloidal distribution of total incident ion fluences obtained by Langmuir probe array installed at the same poloidal location of the tungsten-coated tiles. Deuterium retention in the tungsten-coated tiles was poloidally uniform with a value of $\sim 10^{22}$ D/m². In the case of tungsten-coated samples irradiated by plasma simulators,

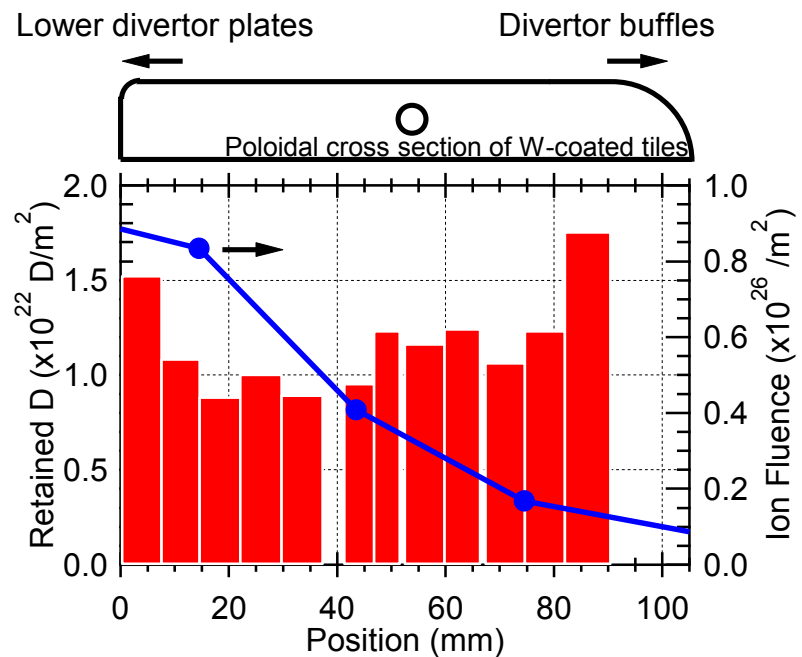


FIG. 2. Poloidal distribution of retained deuterium in the tungsten-coated tiles exposed to JT-60U divertor plasmas obtained by TDS. Total incident ion fluences during the deuterium discharges are also shown with right axis. The origin of the horizontal axis is corresponding to the lower tile edge of the tungsten-coated tiles.

deuterium retention was $\sim 5 \times 10^{20}$ D/m² [5,6] where similar ion flux density, ion fluence and sample temperature. The typical experimental conditions for JT-60U divertor region and the plasma simulators are compared in Table 1 with typical deuterium retention. The deuterium retention in tungsten coated tiles exposed to JT-60U divertor plasma was more than one order of magnitude higher than that observed from plasma simulators. As shown in Table 1, the incident ion energy of JT-60U divertor plasmas was higher than that of the plasma simulators. Deuterium retention in tungsten is increased with the incident ion energy under identical experimental conditions [7]. When the sample temperature is 300 K, deuterium retention in tungsten irradiated by 250 eV deuterium ion beams ($\sim 1.3 \times 10^{20}$ D/m²) was ~ 1.5 times higher than that irradiated by 100 eV deuterium ion beams ($\sim 1.9 \times 10^{20}$ D/m²). This ratio decreases with increase in incident ion fluences and sample temperature [7]. Even if the influence of the ion energy difference was considered, the deuterium retention difference is too large between the tiles exposed to JT-60U divertor plasmas and the samples irradiated by plasma simulators.

Table 1. Comparison of experimental conditions for JT-60U divertor plasmas and plasma simulators

	JT-60U div. plasma	Plasma simulators [5,6]
Ion energy	~ 250 eV	100 eV
Flux density	10^{21} - 10^{22} /m ² s	5×10^{21} - 10^{22} D/m ²
Fluence	10^{25} - 10^{26} /m ²	10^{25} - 10^{26} D/m ²
Sample tem.	~ 700 K	~ 700 K
D retention	$\sim 10^{22}$ D/m ²	$\sim 5 \times 10^{20}$ D/m ²

Higher D retention in the tungsten-coated tiles exposed to JT-60U divertor plasmas is ascribed to carbon accumulated in the tungsten coating. Figure 3 shows depth profiles of deuterium and carbon concentration, and D/C ratio in the tungsten coating obtained by the SIMS depth profiling. The deuterium and carbon signal intensity was calibrated by the TDS and the XPS data obtained from similar measurement points. The carbon concentration was highest near the surface with $\sim 4 \times 10^{28}$ C/m⁻³ and was decreased

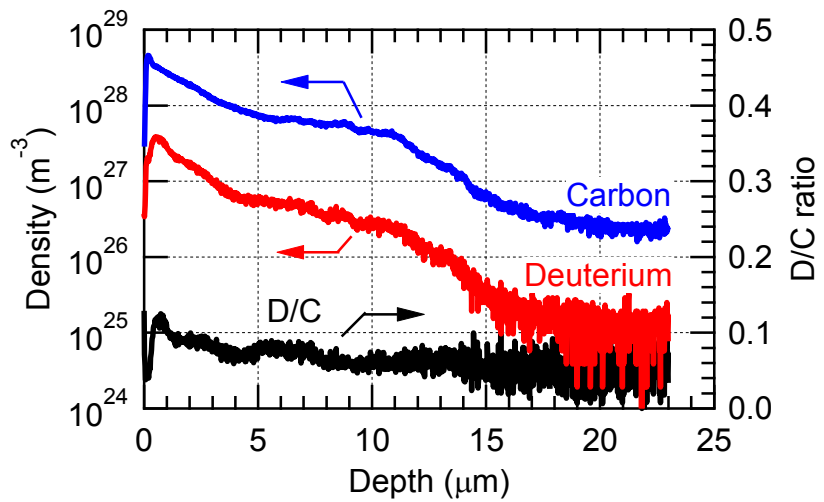


FIG. 3. Depth profiles of deuterium and carbon concentration measured by SIMS depth profiling. D/C ratio in tungsten coating exposed to JT-60U divertor plasmas are also shown with right axis.

with increase in the depth. No clear carbon deposition on the tungsten coating was observed from cross-sectional views of a scanning electron microscope (SEM). Hence, the carbon detected by the SIMS depth profiling was attributed carbon distribution in the tungsten coating. The depth profile of deuterium concentration was similar to that of carbon, resulting

D/C nearly constant throughout the tungsten coating. These results suggest that implanted deuterium is predominantly trapped by the carbon in the tungsten coating. The D/C ratio evaluated beyond $\sim 5 \mu\text{m}$ deep was 0.06 ± 0.02 . D/C ratio in carbon codeposits was 0.2 ± 0.1 [8] formed at similar temperature to the tungsten coating. The D/C ratio in the tungsten coating was only two to four times lower than that in carbon codeposits.

As shown in Fig. 3, carbon was accumulated in the tungsten coating exposed to JT-60U divertor plasmas. The following three carbon sources are considered: (1) implantation of carbon eroded from carbon armor tiles during plasma discharges, (2) thermal diffusion of carbon from the CFC substrate through the Re/W multi-interlayer during plasma discharges, (3) contamination of carbon during the manufacturing process of the tungsten coating.

The carbon concentration in the tungsten coating was decreased with increase in depth, see Fig. 3. If the carbon is diffused from the CFC substrate, carbon concentration in the tungsten coating is decreased toward the surface. Hence, carbon diffusion from the CFC substrate is not dominant process for carbon accumulation near the surface.

To examine amount of the carbon accumulated during the manufacturing process, carbon concentration near the surface was obtained from virgin samples. Figure 4 shows the depth profile of carbon concentration near the surface of virgin samples obtained from the XPS depth profiling. For comparison, the data obtained from the tungsten coating exposed to JT-60U divertor plasmas is also shown. The carbon concentration at the top surface was $\sim 15\%$ and was decreased with increase in depth. The carbon source in the virgin sample is considered to be due to contamination of carbon during the manufacturing process and long-term storage in air atmosphere. The carbon concentration in the tungsten coating after the plasma exposure was increased compared to the virgin samples. Therefore, the dominant carbon source in the tungsten coating exposed to JT-60U divertor plasmas is the implantation of carbon ions eroded from carbon armor tiles during plasma discharges.

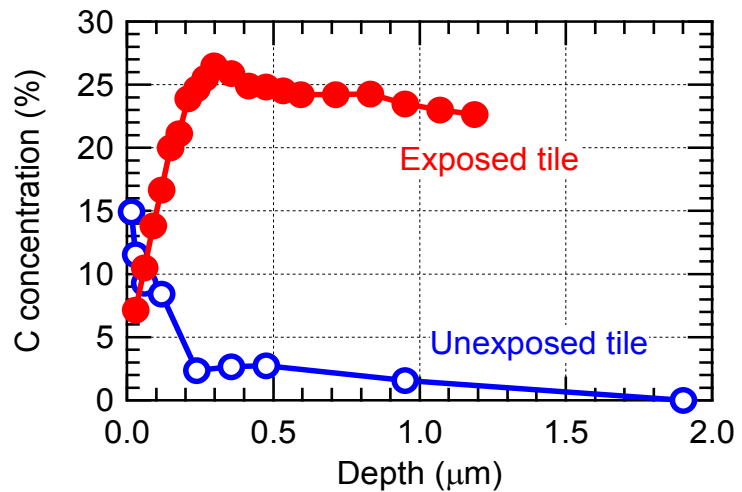


FIG. 4. Depth profiles of carbon concentration in tungsten coating measured by XPS depth profiling before and after exposure to JT-60U divertor plasmas.

As shown in fig. 3, the carbon concentration at $\sim 0.2 \mu\text{m}$ deep, $\sim 4 \times 10^{28} \text{ C/m}^3$, was similar to carbon density of the carbon codeposits, $\sim 0.91 \text{ g/cm}^3$, formed in the inner divertor plates in JT-60U [9]. The carbon concentration in deeper region of the tungsten coating would be increased up to similar concentration of near the surface with plasma discharge duration. With increase in carbon concentration in deeper region, the deuterium retention would also be increased with the constant D/C ratio of 0.06 ± 0.02 . However, it is possibility that this D/C ratio in the tungsten coating depend on the temperature such as carbon codeposits.

4. Deuterium desorption

To examine deuterium trapping site in the tungsten coated tiles exposed to JT-60U divertor plasmas, thermal desorption spectrum of deuterium was obtained by TDS. Figure 5 shows thermal desorption spectrum of deuterium from the tungsten-coated tiles exposed to JT-60U divertor plasmas. The deuterium was desorbed over a temperature from 500 K to 1373 K. The thermal desorption spectrum had at least four inflection points at ~ 730 K, ~ 870 K, ~ 980 K and ~ 1290 K. These inflection points indicate that the thermal desorption spectrum consists of more than four peaks. As a first step of analysis, the thermal desorption spectrum was fitted by a several Gaussian distributions. This desorption spectrum was fitted by ~ 6 Gaussian distributions which were overlapped each other. These multiple desorption peaks indicate that multi-trapping sites for deuterium exist in the tungsten-coated tiles exposed to JT-60U divertor plasmas. However, it was difficult to specify the trapping sites corresponding to each desorption peak. To examine the deuterium trapping in carbon in tungsten-coated tiles, thermal desorption spectrum of deuterium were obtained from the tungsten-coated samples irradiated with deuterium ions.

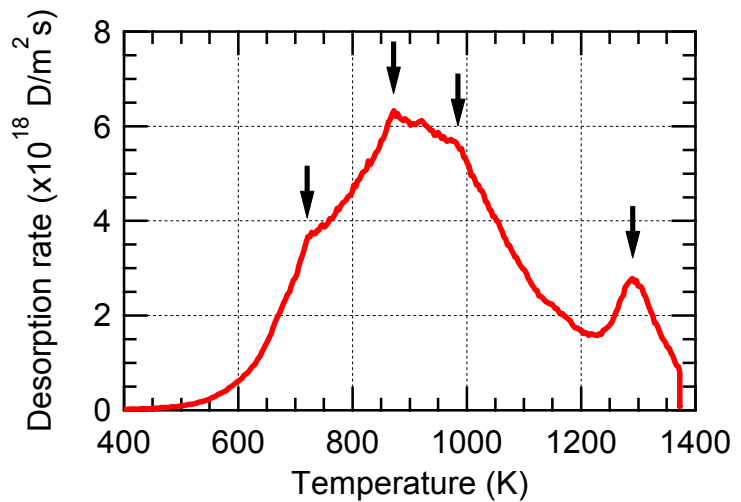


FIG. 5. Thermal desorption spectrum of deuterium obtained from tungsten-coated tiles exposed to JT-60U divertor plasmas. The arrows indicate inflection points.

Deuterium ion irradiation was performed using high flux ion irradiation device HiFIT [3]. The samples were obtained from virgin tungsten-coated tiles manufactured for JT-60U. Before the deuterium ion irradiation, the samples were heated to 1273 K in a vacuum to remove residual gas in tungsten coating. Deuterium ion energy was 1.0 keV. Deuterium ion flux density and fluence was set to $\sim 1.0 \times 10^{20}$ D/m² and $\sim 1.3 \times 10^{24}$ D/m², respectively. Sample temperature was kept to 500 K.

Figure 6 shows a thermal desorption spectrum of deuterium obtained by TDS. A single desorption peak at the temperature of ~ 610 K was observed. This single peak indicates that only one trapping site exists in the tungsten-coated samples irradiated with deuterium ions.

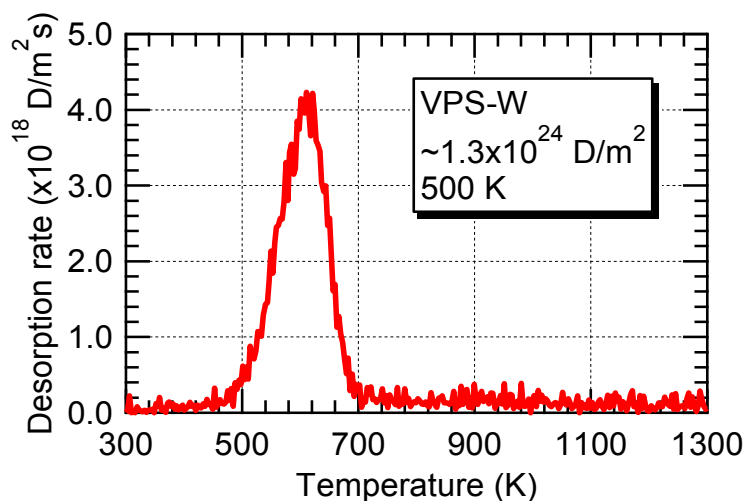


FIG. 6. Thermal desorption spectrum of deuterium for irradiation fluence of $\sim 1.3 \times 10^{24}$ D/m² and sample temperature at 500 K.

To examine the deuterium trapping energy in the tungsten-

coated samples, the deuterium thermal desorption from the samples was simulated by TMAP7 (Tritium Migration and Analysis Program, version 7) code [10]. The deuterium diffusion coefficient in tungsten, $D_0 = 2.9 \times 10^{-7} \exp(-0.39 \text{ eV}/kT) \text{ m}^2/\text{s}$, the recombination coefficient and the dissociation coefficient on the surface of tungsten coating, $K_r = 3.2 \times 10^{-15} \exp(-1.16 \text{ eV}/kT) \text{ m}^4/\text{s}$ and $K_d = 1.09 \times 10^{34} \exp(-3.24 \text{ eV}/kT) \text{ m}^4/\text{s}$, respectively, were used in this simulation. The depth distribution of trapped deuterium was given from experimental results obtained from the SIMS depth profiling. Deuterium trapping site in the tungsten-coated samples was assumed to be filled with deuterium atoms [10]. The deuterium trapping energy was scanned to fit the thermal desorption spectrum. Figure 7 shows thermal desorption spectrum and simulation fit. The trapping energy of $\sim 1.28 \text{ eV}$ fitted the experimental result. This trapping energy is similar to that of monovacancies, $1.34 \pm 0.05 \text{ eV}$, obtained from simulation of deuterium thermal desorption from single crystalline tungsten irradiated at 300 K [11].

The monovacancies in tungsten become mobile at above $\sim 600 \text{ K}$ and agglomerate with other vacancy type defects to form large defects such as vacancy clusters and voids or annihilate at defect sinks, for example, dislocations, grain boundaries and surface [12,13]. Since the tungsten-coated samples were annealed at 1273 K in the vacuum before the deuterium ion irradiations, no monovacancies exist in the tungsten coating but large defects such as vacancy clusters and voids would remain.

The maximum energy of knocked on tungsten atoms produced by 1.0 keV deuterium ions ($\sim 43 \text{ eV}$) is higher than the displacement threshold energy ($\sim 40 \text{ eV}$) for tungsten [14]. Hence, ion-irradiation-induced defects are formed in the tungsten coating during the deuterium ion irradiations. The ion-irradiation-induced defects produced by collision cascade in tungsten are mainly monovacancies and interstitials with few defect clusters [13,15]. Since monovacancies of tungsten are not mobile at 500 K [12,13], vacancy clusters and voids would not formed during deuterium ion irradiations. Monovacancies and voids were also formed in single crystalline and polycrystalline tungsten well beyond the ion range [11,16]. Although mechanism of defect formation beyond the ion range is unknown, these types of defects would also be formed in the tungsten coating during the deuterium ion irradiations. Therefore, the main trapping sites for deuterium in the tungsten coating irradiated at 500 K is monovacancies formed by the deuterium ion irradiations.

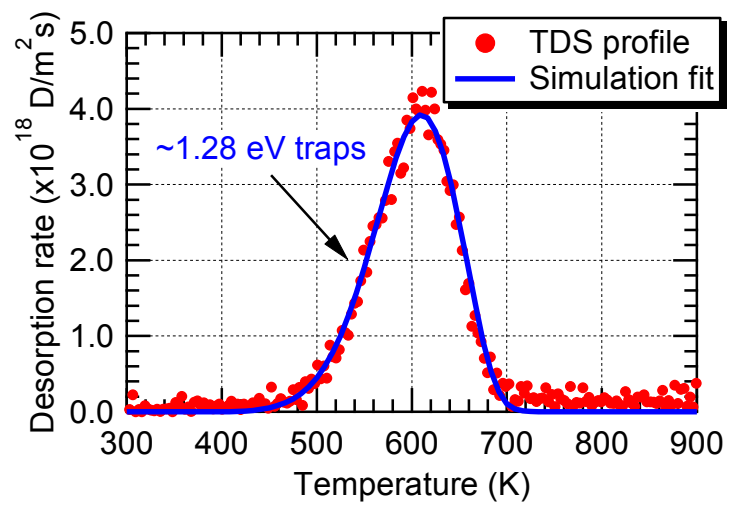


FIG. 7. Thermal desorption profile and simulation fit for irradiation fluence of $\sim 1.3 \times 10^{24} \text{ D/m}^2$ and sample temperature at 500 K .

As shown in Fig. 5, the thermal desorption spectrum of deuterium from the tungsten-coated tiles exposed to JT-60U divertor plasmas has no desorption peak or a small peak at around $\sim 610 \text{ K}$ which was observed from the ion irradiated tungsten-coated samples. Hence, little deuterium would be trapped at the monovacancies in the tungsten coating exposed to JT-60U divertor plasmas. Typical temperature of the tungsten coating after the plasma exposure was $\sim 700 \text{ K}$. Temperature dependence of deuterium retention in polycrystalline and single

crystalline tungsten were obtained from ion irradiation experiments. These results showed that no deuterium retention observed at sample temperature above 700 K [17,18]. Little deuterium retention at the monovacancies in the tungsten coating is consistent to the experimental results of Ref. [17,18]. However, effects of carbon on deuterium desorption have to be considered. Deuterium diffusion and recombination at tungsten surface is delayed by carbon accumulated near the surface. The thermal desorption peak of the deuterium trapped by the tungsten monovacancies would be shifted to higher temperature due to the carbon accumulated near the surface of the tungsten-coated tiles exposed to JT-60U divertor plasmas. To examine thermal desorption spectrum of the deuterium trapped by the monovacancies in tungsten-coated samples, deuterium and carbon mixed ion irradiation experiments is prepared.

6. Conclusion

Deuterium retention and desorption characteristics in tungsten-coated tiles exposed to JT-60U divertor plasmas were observed with surface analysis. Deuterium retention in tungsten-coated tiles were poloidally uniform at $\sim 10^{22}$ D/m² which was more than one order of magnitude higher than that observed from laboratory experiments. Higher deuterium retention in tungsten-coated tiles was due to the deuterium trapping to the carbon accumulated in the tungsten coating. The main carbon sources in the tungsten coating were irradiation of carbon particles eroded from carbon armor tiles during plasma discharges. The D/C ratio in the tungsten coating was 0.06 ± 0.02 which was 1/2-1/4 compared to that in carbon codeposits formed at similar temperature to the tungsten coating. Although multiple trapping sites for deuterium in tungsten-coated tiles were seen, little deuterium retention at the monovacancies in the tungsten coating was observed.

From the results of present work, simultaneous use of carbon and tungsten coating would be enhance tritium retention in tungsten coating up to similar level of carbon codeposits since irradiated tritium ions are trapped by carbon accumulated in tungsten coating used in future DT fusion devices.

References

- [1] Golubeva A.V. et al Hydrogen retention in plasma-sprayed tungsten, in: Hydrogen in Matter: A Collection from the Papers Presented at the 2nd Int. Symp. on Hydrogen in Matter; ISOHIM, AIP Conference Proceedings **vol. 837** (New York: American Institute of Physics) (2006).
- [2] Luo G.-N., et al., Nucl. Instrum. Meth. Phys. Res. B **276** (2009) 3041.
- [3] Ueda Y., et al. Nucl. Fusion **44** (2004) 62.
- [4] Fukumoto M., et al., J. Plasma Fusion Res. SERIES **9** (2010) 369.
- [5] Tokunaga K., et al., J. Nucl Mater. **307-311** (2002) 126.
- [6] Tokunaga K., et al., J. Nucl Mater. **337-339** (2005) 887.
- [7] Tian Z., et al., J. Nucl. Mat. **399** (2010) 101.
- [8] Roth J., et al., J. Nucl. Mater. **390-391** (2009) 1.
- [9] Ishimoto Y., et al., J. Nucl. Mater. **350** (2006) 301.
- [10] G.R. Longhurst, D.F. Holland, J.L. Jones, B.J. Merrill, TMAP4: Tritium Migration Analysis Program, Description and User's Manual, INEL report, EGG-FSP-10315, EG & Idaho Inc. (1992).
- [11] Poon M., et al., J. Nucl. Mater. **374** (2008) 390.
- [12] Eleveld H. and van Veen A. J., Nucl. Mater. **212-215** (1994) 1421.
- [13] Debelle A., et al., J. Nucl. Mater. **376** (2008) 216.
- [14] Jung P. 1991 Atomic Defects in Metals (Landolt-Bornstein New Series III/25) ed H. Ullmaier (Berlin: Springer).

- [15] Caturla M.J., et al., J. Nucl. Mater. **296** (2001) 90.
- [16] Alimov V.Kh., et al., J. Nucl. Mater. **337-339** (2005) 619.
- [17] Haasz A. A., et al., J. Nucl. Mater. **258-263** (1998) 889.
- [18] Poon M. et al., J. Nucl. Mater. **313-316** (2003) 199.